Vietnam Journal of Catalysis and Adsorption
Tạp chí xúc tác và hấp phụ Việt Nam

https://jca.edu.vn

Enhancing epoxy adhesives with CNTs/Gr hybrid for advanced spacecraft applications

To Anh Duc[1,*], Phan Ngoc Minh[2], Bui Hung Thang[3]

[1] *Vietnam National Space Center, Vietnam Academy of Science and Technology, 18 Hoang Quoc Viet, Hanoi, Vietnam*
[2] *Graduate School of Science and Technology, Vietnam Academy of Science and Technology, 18 Hoang Quoc Viet, Hanoi, Vietnam*
[3] *Institute of Materials Science, Vietnam Academy of Science and Technology, 18 Hoang Quoc Viet Street, Hanoi, Vietnam*
** Email: taduc@vnsc.org.vn*

ARTICLE INFO

Received: 03/02/2025
Accepted: 22/03/2025
Published: 30/03/2025

Keywords:
Graphene Nanoplatelets; CNTs; Functionalization; Young's modulus; Flexural modulus.

ABSTRACT

The growing demand for advanced materials in small satellite applications, particularly Carbon Fiber Reinforced Polymers (CFRP), underscores the need for innovations in composite components. As epoxy resin forms a key matrix in CFRP, enhancing its properties is crucial for meeting the rigorous demands of space technology. A promising approach involves using functionalized Carbon Nanotubes (CNTs-OH) and Graphene (Gr-COOH) as hybrid fillers. Functional groups improve dispersion, interfacial bonding, and minimize agglomeration within the epoxy matrix, overcoming traditional limitations. Remarkably, these hybrids offer mechanical enhancements comparable to methods like Chemical Vapor Deposition (CVD), while simplifying processing and enabling scalability. Their compatibility with epoxy ensures consistent performance and manufacturability. These functionalized systems represent a significant step toward lightweight, durable, and high-strength materials suitable for extreme environments, aligning with the broader goal of developing advanced CFRP for next-generation small satellites.

Introduction

The aerospace industry demands materials with exceptional mechanical properties to ensure the structural integrity and reliability of satellites operating in extreme environments [1-5]. Satellites endure significant mechanical stress during launch, such as high g-forces, as well as exposure to harsh orbital conditions, including temperature fluctuations, radiation, and micro-meteoroid impacts [6-9]. These challenges necessitate the development of advanced composite materials that can withstand such extremes while maintaining lightweight and high-performance characteristics.

Epoxy resins, widely used as structural adhesives and matrices in composite materials, provide good mechanical properties, thermal stability, and ease of processing. However, conventional epoxy systems are often inadequate in meeting the stringent requirements of modern satellite applications. To address this limitation, nanomaterials such as Carbon Nanotubes (CNTs) and Graphene (Gr) have emerged as promising reinforcements due to their remarkable mechanical, thermal, and electrical properties [10-13]. When functionalized, these materials not only enhance the dispersion within the matrix but also improve interfacial bonding, further optimizing the composite's mechanical performance.

https://doi.org/10.62239/jca.2025.011

Over the past two decades, significant progress has been made in the incorporation of nanomaterials like Graphene and CNTs into epoxy matrices to enhance mechanical properties. Carbon nanotubes, with their high aspect ratio and superior tensile strength, have shown remarkable potential in reinforcing epoxy, leading to improved crack resistance and toughness. Similarly, Graphene, owing to its two-dimensional structure and large surface area, has been extensively studied for its ability to enhance the in-plane stiffness and strength of epoxy composites. These advancements have paved the way for their adoption in various fields, including automotive, construction, and aerospace sectors. However, these studies have largely focused on either Graphene or CNTs individually [14-20], with limited exploration of their combined use as a hybrid reinforcement system.

The combination of CNTs and Graphene in an epoxy matrix introduces an unprecedented opportunity to synergize their complementary properties, creating a material with superior performance characteristics. For applications such as satellite housing [21-23], where both Young's and flexural modulus are critical, the hybridization of CNTs and Graphene holds immense potential. This approach leverages the crack-bridging and toughness-enhancing properties of CNTs alongside the stiffness and load transfer efficiency of Graphene, resulting in a composite material that exceeds the performance limitations of single-reinforcement systems. Despite the promising potential of this combination, its application in space-related technologies has not been extensively investigated, making the present study a novel contribution to the field. By addressing this gap, the current work seeks to develop a high-performance hybrid composite specifically tailored for the extreme conditions encountered in satellite applications.

Table 1: Increase in Young's modulus for different filler combinations

Ref.	Fillers (ratio)	Mixing method	Increase in Young's modulus
24	CNTs/Gr (1:1)	Mechanical mixing	40%
24	CNTs/Gr (1:1)	CVD	22%
25	CNTs/ Gr (2:8)	Solution blending	13.3%
26	CNTs/GO (1:3)	Solution blending	13.3%

However, as indicated in the data, there is a limited number of previous studies that have researched the combination of Graphene and CNTs to improve the mechanical properties of epoxy resin [24-26]. While this hybrid filler system demonstrates significant improvements in Young's modulus (e.g., up to 40% improvement with CVD), the research is sparse and largely constrained to a few mixing methods which are not suitable for spacecraft applications, as they cannot provide the level of homogeneity, high-performance bonding, and structural reliability required for extreme space environments. Thus, there is a critical need to explore other techniques, such as chemical functionalization and ultrasonic dispersion, to fully harness the potential of CNTs/Gr hybrid composites for aerospace-grade applications.

The hybrid of functionalized CNTs and Graphene also provides added advantages, such as lightweight construction and the potential for improved thermal stability and radiation resistance-critical properties for space environments. The combination of these materials ensures superior reinforcement and multifunctionality, making the hybrid system an excellent candidate for satellite shells and other aerospace applications [27-30].

Experimental

The epoxy resin used is D.E.R. 331 from Dow Chemicals (USA), a non-volatile resin with high rigidity, excellent adhesion, and good chemical resistance. The hardener used is D.E.H. 24, which complements the epoxy resin to form a robust curing system, enhancing its mechanical and chemical properties. Some properties of D.E.R. 331 and D.E.H. 24 are as follows:

Table 2: Properties of D.E.R. 331 Epoxy Resin and D.E.H. 24 Hardener

	D.E.R. 331	D.E.H. 24
Water content	700 ppm max	0.5 wt% max
Equivalent weight	182–192 g/eq (Epoxide)	24 g/eq (Amine hydrogen)
Viscosity at 25°C	11,000–14,000 mPa·s	19.5–22.5 mPa·s
Specific gravity at 25°C	1.16 g/ml	0.981 g/ml
Color (Platinum-Cobalt scale)	75 max	50 max
Shelf life	24 months	24 months

https://doi.org/10.62239/jca.2025.011

Graphene Nanoplatelets (ACS Material) were functionalized with carboxyl groups by treating in a solution of nitric acid and sulfuric acid (HNO_3:H_2SO_4, 1:3) at 70°C for 5 hours under continuous magnetic stirring. After that, the Graphene was thoroughly rinsed with distilled water and dispersed in ethylene glycol using ultrasonication for 30 minutes to form a Gr–COOH dispersion at a concentration of 1 g/L.

Separately, multi-walled CNTs (ACS Material) were functionalized by subjecting them to the same acid treatment (HNO_3:H_2SO_4, 1:3) at 70°C for 5 hours. Afterward, they were cleaned with distilled water and dried under vacuum for 24 hours. The dried CNTs–COOH was reacted with thionyl chloride ($SOCl_2$) at 60°C for 6 hours, resulting in CNTs–COCl. The reaction product was filtered, washed with Tetrahydrofuran (THF), and rinsed with distilled water. The CNTs–COCl was then dispersed in Ethylene Glycol and stirred at 120°C for 8 hours. After additional washing with THF and distilled water, the CNTs–OH dispersion was prepared by ultrasonication in Ethylene Glycol for 30 minutes to reach a concentration of 1 g/L.

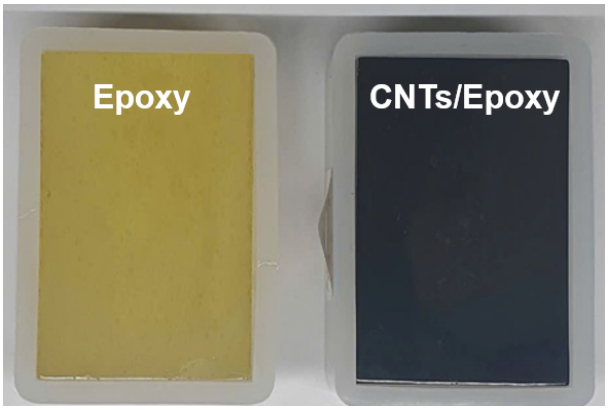

Figure 1: Improved dispersibility of carbon nanomaterials in the matrix after effective functionalization

To prepare the CNTs/Gr hybrid dispersion, equal volumes of Gr-COOH and CNTs-OH dispersions were mixed at a 1:1 ratio, ultrasonicated for 45 minutes in an ice-water bath to ensure homogeneity and adjusted to target weight percentages of 0.05–0.45 wt% by diluting or concentrating the mixtures for precise composition control. This hybrid dispersion was then added to D.E.R. 331 epoxy resin and mechanically stirred at 300 rpm for 30 minutes to promote uniform distribution. The resulting mixture underwent ultrasonication in an ice-water bath for an additional 20 minutes to enhance dispersion and minimize agglomeration. Following this, D.E.H. 24 hardener was introduced to the epoxy-hybrid mixture at a 100:12 weight ratio (resin:hardener) and blended at 500 rpm for 10 minutes to ensure homogeneity. Finally, the mixture was degassed under vacuum at 50 mbar for 15 minutes to eliminate air bubbles, ensuring a smooth and consistent formulation suitable for further processing.

To measure the mechanical properties of the two-component epoxy material reinforced with the CNTs/Gr hybrid, a mold as shown in Figure (2a) was fabricated with dimensions meeting the Young's modulus testing standard TCVN 4501. Liquid epoxy resin was poured into the mold and cured in an oven for 24 hours. The material sample was then removed from the mold (pre-coated with a non-stick layer) and its mechanical properties were measured using the AGX-50k NVD multifunctional testing machine at Institute of Tropical Technology. To ensure accuracy, three identical material samples were prepared for each measurement, and the recorded value was taken as the average of the three measurements. Similarly, a mold designed to meet ASTM D790 specifications was prepared for flexural modulus testing using the AGX-50k NVD testing machine.

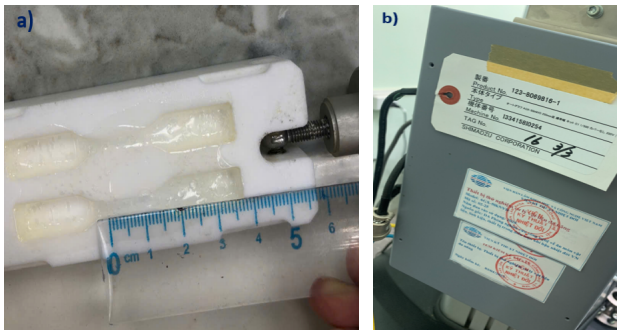

Figure 2: (a) Epoxy casting mold, with dimensions meeting the TCVN 4501 standard;
(b) AGX-50k NVD multifunctional mechanical property testing machine at Institute for Tropical Technology

Results and discussion

Figure (3a) illustrates the FTIR spectra of Gr-COOH, CNTs-OH, and the CNTs/Gr hybrid material, revealing characteristic peaks corresponding to their respective functional groups. For Gr-COOH, the FTIR spectrum reveals characteristic peaks that confirm successful functionalization: a broad band at 3,398 cm^{-1} corresponding to O-H stretching vibrations, a peak at 1,728 cm^{-1} attributed to C=O stretching vibrations, and a band at 1,380 cm^{-1} associated with O-H bending vibrations, with an additional peak at 1,554 cm^{-1}

https://doi.org/10.62239/jca.2025.011

indicating graphitic C=C bonds. These peaks collectively indicate the presence of carboxyl (-COOH) groups on the graphene surface, demonstrating effective functionalization.

In the CNTs-OH spectrum, similar functional groups are detected, such as O-H stretching at 3,398 cm^{-1} and a C=C in-plane vibration at 1,554 cm^{-1}. However, unlike Gr-COOH, the C=O stretching band at 1,728 cm^{-1} is absent, indicating the lack of carboxyl functional groups in CNTs-OH. Instead, the spectrum shows a strong band at 1,637 cm^{-1}, primarily attributed to the C=C stretching vibration of the carbon nanotube structure, rather than C=O.

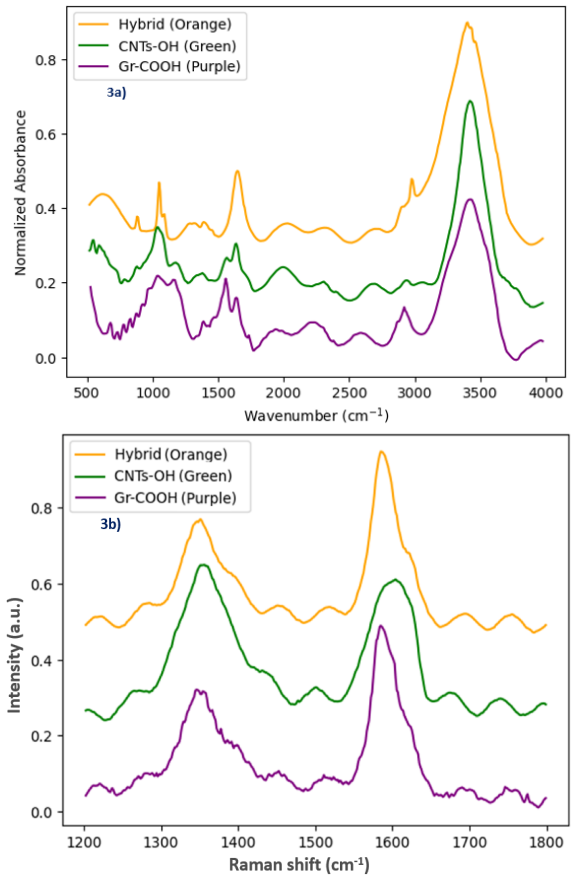

Figure 3: (a) FTIR spectra of the hybrid material, CNTs-OH, and Gr-COOH; (b) Raman spectra of the hybrid material, CNTs-OH, and Gr-COOH

The CNTs/Gr hybrid material exhibits distinctive FTIR features that suggest successful integration between the functional groups of Gr-COOH and CNTs-OH. The prominent peak at 1,637 cm^{-1} corresponds to the C=C stretching vibration, confirming the preservation of the graphitic structure in both Graphene and CNTs. This indicates that the hybrid retains the core sp^2 carbon network essential for its structural integrity. Additionally, the peaks at 1,083 cm^{-1} and 1,045 cm^{-1} are attributed to C-O stretching vibrations, indicating the presence of oxygen-containing linkages. These C-O bonds likely result from the reaction between the carboxyl groups in Gr-COOH and the hydroxyl groups in CNTs-OH, forming bridges that connect the two components. These linkages may integrate the components more cohesively, reducing the number of defect-inducing free functional groups and enhancing the structural order of the hybrid.

Figure (3b) displays the Raman spectra of Gr-COOH, CNTs-OH, and the CNTs/Gr hybrid material, with prominent peaks corresponding to the D band (~1,355 cm^{-1}) and the G band (~1,595 cm^{-1}). The D band reflects the presence of defects, disordered carbon, or sp^3 hybridized carbon atoms, while the G band signifies the stretching vibrations of sp^2-hybridized carbon atoms in the Graphene lattice. The differences in I_D/I_G ratios between Gr-COOH, CNTs-OH, and the CNTs/Gr hybrid material underscore how the synthesis process enhances the structural integrity of the hybrid. CNTs-OH exhibits the highest I_D/I_G ratio of 1.10, indicative of significant defect density due to extensive hydroxyl (-OH) functionalization, which disrupts the graphitic lattice. In contrast, the CNTs/Gr hybrid shows a markedly lower I_D/I_G ratio of 0.60. If the hybrid were simply a physical mixture of Gr-COOH and CNTs-OH, one might expect an I_D/I_G ratio closer to the average of the two components. However, the observed ratio is substantially lower, suggesting that the synthesis process has effectively reduced the overall defect density, which is strongly supported by the distinct FTIR features discussed earlier.

Here are a few key observations we can draw from Table 3:

- CNTs-OH: The Young's and flexural modulus of the composite increase as the concentration of CNTs-OH rises, peaking at 0.4 wt% with values of 2.96 GPa and 2.57 GPa, respectively. This corresponds to an 18.4% increase in Young's modulus and a 16.8% increase in flexural modulus compared to the neat matrix (0.0 wt%). The improvement up to this concentration is attributed to the effective dispersion of CNTs-OH, which enhances load transfer between the matrix and filler. However, beyond 0.4 wt%, both properties decline due to agglomeration of the CNTs-OH, which creates stress concentration points, reducing mechanical performance.

- Gr-COOH: The addition of Gr-COOH leads to a significant improvement in Young's modulus and flexural modulus, with the maximum values of 3.0 GPa and 2.61 GPa observed at 0.2 wt%. This represents a

https://doi.org/10.62239/jca.2025.011

20.0% increase in Young's modulus and an 18.6% increase in flexural modulus compared to the baseline (0.0 wt%). The superior mechanical properties at 0.2 wt% can be attributed to Graphene's exceptional ability to enhance stress transfer and its strong interfacial bonding with the matrix. Beyond this concentration, mechanical properties decrease as Gr-COOH begins to agglomerate, reducing the effective interaction area and causing stress concentrations.

- CNTs/Gr: The hybrid system of CNTs and Graphene (1:1 wt%) exhibits the greatest mechanical enhancements, with Young's modulus reaching 3.48 GPa and flexural modulus peaking at 2.95 GPa at 0.3 wt%, representing a 39.2% and 34.1% increase, respectively. This improvement is attributed to the synergistic effect between CNTs and Graphene, which enhances stress distribution and load transfer within the epoxy matrix.

Table 3: Mechanical Properties (in GPa) of Epoxy Composites with CNTs–OH, Gr–COOH, and CNTs/Gr hybrid at varying concentrations

Wt%	Young's modulus (CNTs-OH)	Flexural modulus (CNTs-OH)	Young's modulus (Gr-COOH)	Flexural modulus (Gr-COOH)	Young's modulus (hybrid)	Flexural modulus (hybrid)
0.0	2.5	2.2	2.5	2.2	2.5	2.2
0.05	2.55	2.24	2.58	2.29	2.63	2.28
0.15	2.65	2.31	2.83	2.47	2.88	2.47
0.2	-	-	**3.0**	**2.61**	3.10	2.61
0.25	2.75	2.41	-	-	3.30	2.82
0.3	-	-	2.97	2.58	**3.48**	**2.95**
0.35	2.88	2.51	-	-	-	-
0.4	**2.96**	**2.57**	2.92	2.54	3.38	2.90
0.45	2.90	2.53	2.88	2.50	3.24	2.64

Mechanically, CNTs act as bridging elements, reducing crack propagation and enhancing fracture resistance, while Graphene improves stiffness and in-plane load transfer due to its high modulus. Their combined presence forms a reinforcement network, reducing stress concentrations and ensuring uniform mechanical enhancement.

However, beyond 0.3 wt% concentration, a decline in mechanical properties is observed, attributed to the agglomeration of CNTs and Graphene within the matrix. At higher filler loadings, Van der Waals forces cause nanomaterials to aggregate, reducing the effective interfacial contact area and leading to defects and stress concentration sites. This behavior mirrors the limitations seen in individually reinforced systems, where excessive filler loading leads to a deterioration of dispersion quality, ultimately compromising mechanical efficiency.

The study of mechanical reinforcement through the addition of CNTs-OH, Gr-COOH, and CNTs/Gr hybrids demonstrates the significant potential of nanofillers in enhancing Young's and flexural modulus. Each material system exhibits a clear saturation point, beyond which mechanical properties decline due to agglomeration. The CNTs-OH system shows optimal performance at 0.4 wt%, Gr-COOH at 0.2 wt%, and the CNTs/Gr hybrid at 0.3 wt%, with the hybrid system delivering the highest percentage improvements in Young's (39.2%) and flexural (34.1%) modulus.

Conclusion

The exceptional performance of the hybrid system can be attributed to the functionalization of both CNTs and Graphene, which enhances interfacial bonding, dispersion, and stress transfer within the matrix. This functionalization achieves a similar level of mechanical improvement to chemical vapor deposition (CVD), approximately 40%, but with several distinct advantages. Unlike CVD, which requires high temperatures, complex equipment, and lengthy processing times, the functionalized hybrid system relies on scalable, room-temperature methods such as solution blending and ultrasonic dispersion. These techniques are not only cost-effective but also ensure higher compatibility with polymer matrices, avoiding the thermal degradation of the resin system that can occur with CVD.

https://doi.org/10.62239/jca.2025.011

Moreover, the CNTs/Gr hybrid system is inherently more versatile and adaptable to various applications. While CVD often produces rigid and uniform coatings, the hybrid approach allows precise tailoring of the filler distribution and concentration within the matrix, enabling the creation of multifunctional composites. For space applications, this adaptability is crucial, as it provides the ability to optimize mechanical, thermal, and electrical properties for specific mission requirements. The hybrid system's lightweight nature, combined with its superior manufacturability and performance under extreme conditions, positions it as a more practical and sustainable alternative to CVD for aerospace-grade composites.

Future work will focus on incorporating this hybrid into CFRP to develop stronger, lightweight housing and structural components for spacecraft, leveraging its improved mechanical properties. The data in this study demonstrates that the inclusion of CNTs, Graphene, and their hybrid reinforcements significantly enhances Young's modulus and flexural modulus, making these materials highly suitable for structural applications in small satellites. Given the extreme mechanical stresses encountered during launch, orbital operation, and re-entry, further optimization is needed to maximize strength, toughness, and durability while maintaining low weight and manufacturability. Additionally, refining polymer-matrix interactions and exploring alternative hybrid compositions could further enhance mechanical stability and fatigue resistance for aerospace applications.

Beyond mechanical improvements, future research should also focus on enhancing EMI shielding capabilities and ensuring long-term performance under extreme space conditions, such as vacuum, radiation exposure, and temperature variations. EMI shielding is crucial for protecting satellite electronics from cosmic radiation and external electromagnetic disturbances. Optimizing the dispersion and alignment of CNTs and Graphene can improve conductive networks, leading to better shielding effectiveness while preserving mechanical integrity. Scaling up production and integrating these materials into aerospace manufacturing will be key to realizing their full potential in next-generation spacecraft and satellite technologies.

Acknowledgments

This research is funded by Vietnam Academy of Science and Technology (VAST) under grant number VAST01.03/24-25.

References

1. R. R. Krishnamoorthy, D. Marius, Appl. Catal. A 121 (2025) 159–206.https://doi.org/10.1016/B978-0-443-221187.00007-5
2. H. Djojodihardjo, Acta Astronautica (2024). https://doi.org/10.1016/j.actaastro.2024.05.034
3. J. Yang, Z. Zhu, S. Han, Y. Gu, Z. Zhu, H. Zhang, J. Alloys Compd. 176707 (2024). https://doi.org/10.1016/j.jallcom.2024.176707
4. I. N. Wani, K. Aggarwal, S. Bishnoi, P. Shukla, D. Harursampath, A. Garg, J. Mater. Res. Technol. 138 (2024). DOI:10.20944/preprints202402.0382.v1.
5. J. C. Ince, M. Peerzada, L. D. Mathews, A. R. Pai, A. Al-Qatatsheh, S. Abbasi, N. V. Salim, Adv. Compos. Hybrid Mater. 6(4) (2023) 130. https://doi.org/10.1007/s42114-023-00678-5
6. R. Reda, Y. Ahmed, I. Magdy, H. Nabil, M. Khamis, A. Refaey, G. Abed, Trans. Aerosp. Res. (2023). https://doi.org/10.2478/tar-2023-0016
7. D. V. Breslavs'kyi, S. O. Pashchenko, O. A. Tatarinova, Strength Mater. 51 (2019) 231–239. https://doi.org/10.1007/s11223-019-00069-6
8. J. Shen, H. M. Liu, J. Wang, Math. Biosci. Eng. 19 (2022) 2120–2146. DOI: 10.3934/mbe.2022099
9. A. S. Tsybenko, B. M. Rassamakin, A. A. Rybalka, Strength Mater. 49 (2017) 381–387. https://doi.org/10.1007/s11223-017-9878-0
10. S. Nasir, M. Z. Hussein, Z. Zainal, N. A. Yusof, Mater. 11(2) (2018) 295. https://doi.org/10.3390/ma11020295
11. V. K. Thakur, M. K. Thakur, Chem. Funct. Carbon Nanomater. (2018) 5–13. Warentown (NJ: CRC Press. https://doi.org/10.3390/ma11020295
12. M. Chakraborty, M. S. J. Hashmi, Adv. Mater. Process. Technol. 4(4) (2018) 573–602. https://doi.org/10.1080/2374068X.2018.1484998
13. G. Zhao, X. Li, M. Huang, Z. Zhen, Y. Zhong, Q. Chen, H. Zhu, Chem. Soc. Rev. 46(15) (2017) 4417–4449. https://doi.org/10.1080/2374068X.2018.1484998
14. D. G. Papageorgiou, I. A. Kinloch, R. J. Young, Prog. Mater. Sci. 90 (2017) 75–127. https://doi.org/10.1016/j.pmatsci.2017.07.004
15. Ö. Güler, N. Bağcı, J. Mater. Res. Technol. 9(3) (2020) 6808–6833. https://doi.org/10.1016/j.jmrt.2020.01.077
16. K. Chu, X. H. Wang, Y. B. Li, D. J. Huang, Z. R. Geng, X. L. Zhao, H. Zhang, Mater. Des. 140 (2018) 85–94. https://doi.org/10.1016/j.matdes.2017.11.048
17. V. Khanna, V. Kumar, S. A. Bansal, Mater. Res. Bull. 138 (2021) 111224. https://doi.org/10.1016/j.materresbull.2021.111224
18. K. Chu, F. Wang, X. H. Wang, D. J. Huang, Mater. Sci. Eng. A 713 (2018) 269–277. https://doi.org/10.1016/j.msea.2017.12.080
19. A. Ali, S. S. R. Koloor, A. H. Alshehri, A. Arockiarajan, J. Mater. Res. Technol. 24 (2023) 6495–6521. https://doi.org/10.1016/j.jmrt.2023.04.072

20. Y. Lin, Q. Shi, Y. Hao, Z. Song, Z. Zhou, Y. Fu, J. Wu, Int. J. Mech. Sci. 257 (2023) 108532. https://doi.org/10.1016/j.ijmecsci.2023.108532
21. M. Shifa, F. Tariq, F. Khan, Z. S. Toor, R. A. Baloch, Mater. Res. Express 6(12) (2020) 125629. https://doi.org/10.1088/2053-1591/ab6928
22. T. S. Jang, J. Rhee, J. K. Seo, Acta Astronaut. 117 (2015) 497–509. https://doi.org/10.1016/j.actaastro.2015.09.014
23. T. S. Jang, H. K. Cho, H. S. Seo, W. S. Kim, J. H. Rhee, J. Korean Soc. Aeronaut. Space Sci. 38(12) (2010) 1209–1216. https://doi.org/10.5139/JKSAS.2010.38.12.1209
24. W. Li, A. Dichiara, J. Bai, Compos. Sci. Technol. 74 (2013) 221–227. https://doi.org/10.1016/j.compscitech.2012.11.015
25. L. Yue, G. Pircheraghi, S. A. Monemian, I. Manas-Zloczower, Carbon 78 (2014) 268–278. https://doi.org/10.1016/j.carbon.2014.07.003
26. Y. Li, R. Umer, A. Isakovic, Y. A. Samad, L. Zheng, K. Liao, RSC Adv. 3(23) (2013) 8849–8856. https://doi.org/10.1039/C3RA22300K
27. Sarkar, L., Saha, S., Samanta, R., Sinha, A., Mandal, G., Biswas, A., Das, A., J. Inst. Eng. (India): Ser. D 105(1) (2024) 527–541. https://doi.org/10.1007/s40033-023-00465-y
28. T. Dutta, I. Llamas-Garro, J. S. Velázquez-González, J. Bas, R. Dubey, S. K. Mishra, IEEE Sens. J. (2024). https://doi.org/10.1109/JSEN.2024.3440499
29. M. Etesami, M. T. Nguyen, T. Yonezawa, A. Tuantranont, A. Somwangthanaroj, S. Kheawhom, Chem. Eng. J. 446 (2022) 137190. https://doi.org/10.1016/j.cej.2022.137190
30. C. L. Han, A. L. Zou, G. D. Wang, Y. Liu, N. Li, H. X. Zhang, E. Blackie, Diam. Relat. Mater. 124 (2022) 108953. https://doi.org/10.1016/j.diamond.2022.108953